Enhancement in optical and electrical efficiency of a Si nanocrystal light-emitting diode by indium tin oxide nanowires

Chul Huh, Tae-Youb Kim, Byoung-Jun Park, Eun-Hye Jang, and Sang-Hyeob Kim

IT Convergence Technology Research Laboratory, Electronics and Telecommunications Research Institute, Daejeon 305-350, Republic of Korea, chuh@etri.re.kr

ABSTRACT

We report an enhancement in light emission efficiency form Si nanocrystal (NC) light-emitting diodes (LEDs) by employing indium tin oxide (ITO) nanowires (NWs). The electrical characteristics of Si NC LED with ITO NWs were significantly improved, which was attributed to an enhancement in the current spreading property of the ITO transparent layer and a decrease in the dynamic resistance of the whole Si NC LED. Moreover, light output power and wall-plug efficiency (WPE) from the Si NC LED with ITO NWs were enhanced by 45 and 38 %, respectively. The results presented here can provide a very promising way to significantly enhance the performance of Si NC LED.

Keywords: Si nanocrystal, ITO nanowires, Light-emitting diode, Wall-plug efficiency, Light output power

1 INTRODUCTION

Up to now, enormous researches have been done on searching for a highly efficient Si-based light source to realize the Si nanophotonics [1-3]. Unfortunately, bulk Si shows the poor luminescence efficiency because bulk Si has an indirect band gap. To improve the luminescence efficiency of Si-based light source, Si nanocrystals (NCs) has, therefore, attracted the most attention to fabricate highly efficient light-emitting diodes (LEDs) [4,5]. The quantum efficiency of Si NCs could be significantly improved due to an increase in the possibility of overlapping of electron-hole wave functions, that is, a quantum confinement effect [6]. This implies that Si NCs are of particular interest as a source of highly efficient Si-based LEDs. In addition, Si NCs has been expected as a potential candidate for a Si solar cell with high efficiency due to a carrier multiplication by generation of two or more electron-pairs following the absorption of a single photon [7,8]

In order to synthesize the Si NCs, the Si-rich oxide (SRO) film has been generally applied as the surrounding matrix [9]. The SRO film, however, has disadvantages as the surrounding matrix for the formation of the Si NCs. The electrons would be trapped in localized levels in the band gap of nanocrystals, resulting in an uncontrollable tuning of the emission wavelength of Si NC [10]. In addition, the formation of Si NCs in Si-rich oxide film requires a relatively high annealing temperature after Si implantation into the oxide film. It is generally known that the high operating voltage needs to inject the carriers into Si NCs. This is attributed to a huge tunnel barrier between Si NC and Si-rich oxide film due to a large band gap of Si oxide film (8.5 eV). Therefore, alternative approaches have been conducted to synthesize the Si NCs with an appropriate emission state for quantum confinement effects [11,12].

In our previous result [13], well-organized Si NCs in a silicon nitride films was grown by a conventional plasma enhanced chemical vapor deposition (PECVD) at a relatively low temperature. The results demonstrated that the Si NCs in the silicon nitride films showed a clear quantum confinement effect depending on the size of Si NCs, suggesting that the band gap of Si NCs could be tuned from the near infrared (1.38 eV) to the ultraviolet (3.02 eV) range.

A thin metal film or poly-Si layer has been generally used to inject the carriers into the Si NCs through the surrounding matrix. For a thin metal film, however, the light emitted from the active layer would be easily absorbed at the metal film, resulting in a decrease in the light extraction efficiency. In the case of a poly-Si layer, this layer shows a good electrical property but has the shortcoming of absorption of the emitted light from active layer due to the relatively low band gap of poly-Si. Therefore, the transparent doping layer, which has good electrical property and high transparency for the emitted light, is indispensable for enhancing the efficiency of Si NC LEDs. In the previous result [14,15], our group fabricated the mesa-type Si NC LEDs by applying an amorphous SiC doping layer and an indium tin oxide (ITO) current spreading layer. We obtained a p-n junction diode structure and observed that the electrons that stem from the SiC doping layer could be effectively injected into the Si NC and subsequently recombine radiatively. In addition, we found that an amorphous SiC layer could be used as a doping layer with good electrical property and high transparency.

Recently, surface plasmons (SPs) have attracted significant interest because light emission of LEDs can be greatly improved by an increase in the spontaneous emission rate and internal quantum efficiency (IQE) due to the coupling between SPs and emitter [16-18]. It was reported that the light output power of InGaN/GaN multi-quantum well (MQW) blue LEDs was enhanced by 32.2% due to the strong coupling of QW light emitter and the SPs

of the Ag nanoparticles (NPs) [19]. Lu et al. [20] demonstrated a 2.8-fold enhancement in peak photoluminescence (PL) intensity of InGaN/GaN MQWs due to a QW-SP coupling in Ag-SP LED by employing a periodic 2-dimensional Ag array. Likewise, the IQE of CdSe-based NCs on Au layer was significantly enhanced due to the fact that the electron-hole pairs generated in the NCs coupled to SPs at the interface between the NCs and Au layer [21]. Although these approaches can increase the luminescence efficiency of the emitters, there are additional steps, such as an annealing process to form the metal NPs and patterning process to create the metal array in the LED structure, meaning that the LED fabrication process is a relatively complicated. Therefore, to further improve the performance of a Si NC LED, a conductive electrode layer that can uniformly deliver the electrons into the Si NCs should be addressed. In addition, this layer must have a high transparency to increase the probability of photons escaping from the Si NC LED. In this work, a new technique for improving the optical and electrical properties of Si NC LEDs by employing ITO nanowires (NWs) was investigated.

2 EXPERIMENTAL

The The Si NCs embedded in a silicon nitride (SiN_x) matrix with a thickness of 50 nm was grown by a conventional plasma-enhanced chemical vapor deposition (PECVD), in which Ar-diluted 10% SiH_4 and NH_3 were used as the sources of reactants. Silicon wafers doped with boron (~10^{18} cm^{-3}) were used as substrates. The plasma power, chamber pressure, and substrate temperature for the growth were fixed at 5 W, 500 mTorr, and 250°C, respectively. The flow rate of SiH_4 and NH_3 gases was 50 and 10 sccm, respectively. No postannealing process was performed to form the Si NCs into the SiN_x matrix after the growth. Amorphous SiC film (50 nm) doped with a P were deposited on the SiN_x layer with Si NCs at 300°C by a PECVD. Ar-diluted 10% SiH_4 and CH_4 gases were employed to grow SiC film. A rapid thermal annealing process at 950°C for 2 min was performed to activate dopant sources into the SiC film. Mesa-type LEDs with an area of 300 μm × 300 μm were fabricated. The SiC and SiN_x films were etched using inductively coupled SF_6/O_2 plasma until the Si layer was exposed. A 100 nm-thick ITO transparent current spreading layer was deposited on the SiC film. The ITO NWs were grown on the ITO transparent current spreading layer by employing a KrF excimer pulsed laser (λ=248 nm) deposition system. The structure of Si NC LED investigated here was ITO NWs/ITO (100 nm)/n-SiC (50 nm)/Si NCs in SiN_x (50 nm)/p^+-Si substrate, which was shown in Fig. 1.

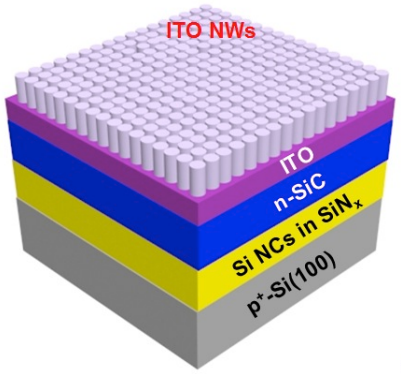

Fig. 1. Structure of Si NC LED with ITO NWs.

The Si NC LED without ITO NWs was also fabricated for comparison. Finally, Ni/Au (20/100 nm) film was deposited for the top and back side contacts via a thermal evaporation. The size of top metal electrode was 80 μm × 80 μm, and the emission area was 8.36 × 10^4 μm^2, respectively. A charge-coupled detector was used for the photoluminescence (PL) measurement with a He–Cd 325 nm laser as the excitation source. The electron concentration of the films was measured at room temperature by using Hall measurement system (Accent HL 5500 Hall System). Current-voltage (*I-V*) characteristics of the LEDs were measured by a HP 4145 semiconductor parameter analyzer. The light output power was measured from the top side of the Si NC LEDs using a calibrated Si photodiode connected to the optical power meter (Newport 818-SL).

3 RESULTS AND DISCUSSION

Figure 2 shows a room-temperature PL spectrum taken from the Si NCs active layer investigated here centered at ~680 nm. The average size and density of Si were ~4 nm and 6.0 × 10^{11} /cm^2, respectively, which was confirmed by a high-resolution transmission electron microscopy [14].

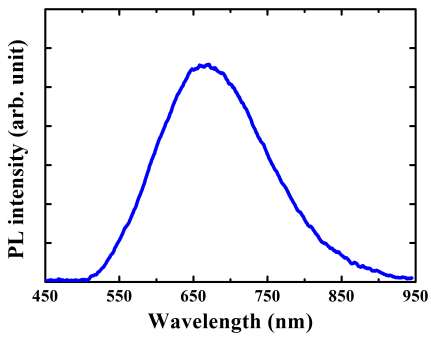

Fig. 2. PL spectrum taken from the Si NCs active layer.

The SEM image of ITO NWs grown at 500 °C is shown in Fig. 3. As the growth temperature of ITO NWs decreased, the ITO NWs were smaller and less uniform in size as compared to those synthesized at 500 °C. The ITO NWs had a tendency to grow perpendicularly above the surface,

even though all of them were not perfectly oriented on the surface.

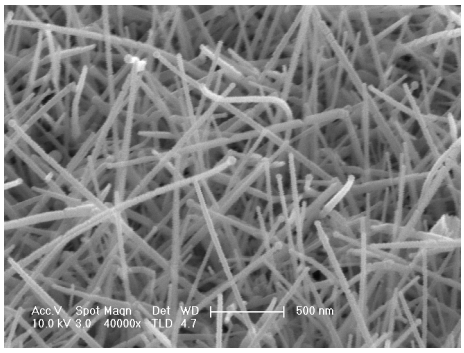

Fig. 3. SEM image of ITO NWs grown at 500 °C.

Figure 4(a) shows the *I-V* curves of Si NC LEDs with and without ITO NWs measured at room temperature, respectively. The electrical property of Si NC LED with ITO NWs was better than that of Si NC LED without ITO NWs. In order to investigate the effect of the ITO NWs on the electrical properties of the Si NC LED, the typical series resistance (R_S) of two Si NC LEDs from the measured *I–V* curves in Fig. 4(a) was calculated. The R_S was calculated from the diode relation of a p-n junction. When the R_S contributes to device behavior, the diode Eq. can be written as, $I = I_0\left(e^{q(V-IR_S)/nkT} - 1\right)$, where I_0 is the prefactor, V the measured voltage, n the ideality factor, respectively [22]. This Eq. can be rewritten as, $I(dV/dI) = IR_S + nkT/q$, indicating that the R_S can be obtained from the slope of this Eq. The calculated R_S is shown in Fig. 4(b). The R_S values were calculated to be 133 and 100 Ω, respectively. The R_S for Si NC LED with ITO NWs was significantly decreased compared with Si NC LED without ITO NWs. This was attributed to an enhancement in the current spreading property of the ITO transparent layer and a decrease in the dynamic resistance of the whole Si NC LED.

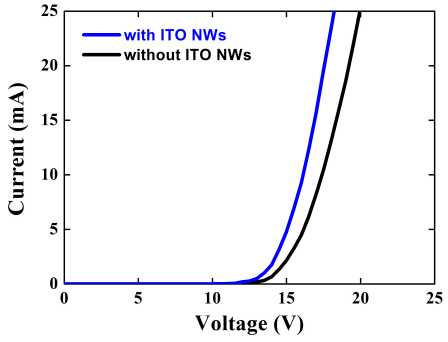

Fig. 4(a). *I-V* curves of Si NC LEDs with and without ITO NWs measured at room temperature, respectively.

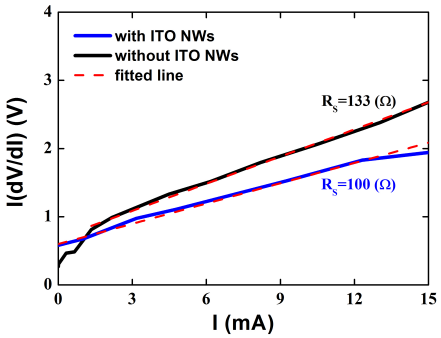

Fig. 4(b). R_S of two Si NC LEDs.

The electroluminescence (EL) spectra were taken from the Si NC LED with ITO NWs as a function of forward current, which was measured at room temperature, as shown in Fig. 5(a). Both PL and EL showed a similar center peak position at 680 nm. This indicates that the PL and EL processes can be related to the same luminescence mechanism that originated from the Si NCs. As shown in Fig. 5(a), the EL intensity increased with the increasing forward current. Fig. 5(b) shows the light output powers of Si NC LEDs with and without ITO NWs as a function of forward voltage, respectively. The light output powers were measured from the topside of the Si NC LEDs by using a Si photodiode connected to an optical power meter (Newport 818-SL). The light output powers of the Si NC LEDs were linearly increased with increasing forward voltage. The light output power for Si NC LED with ITO NWs was improved by 45% compared to that of Si NC LED without ITO NWs. The power efficiency (output power/input power) is very important in real LED applications to reduce power consumption. The wall-plug efficiencies (WPEs), as shown in Fig. 5(c), were calculated based on the *I -V* data and light output power. The WPE of Si NC LED with ITO NWs was improved by 38% compared to that of Si NC LED without ITO NWs.

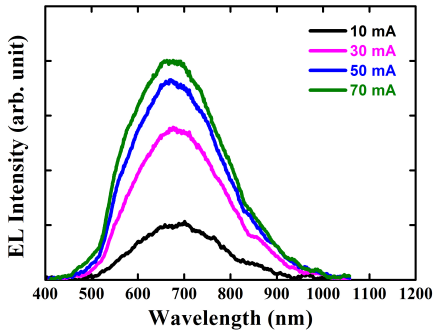

Fig. 5(a). EL spectra of Si NC LED with ITO NWs as a function of current.

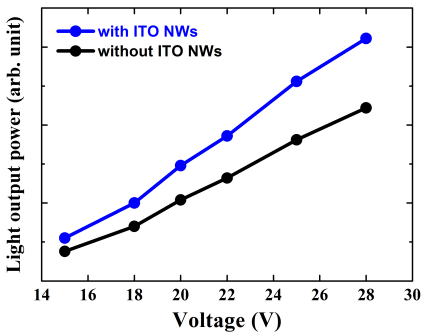

Fig. 5(b). Light output powers of Si NC LEDs with and without ITO NWs.

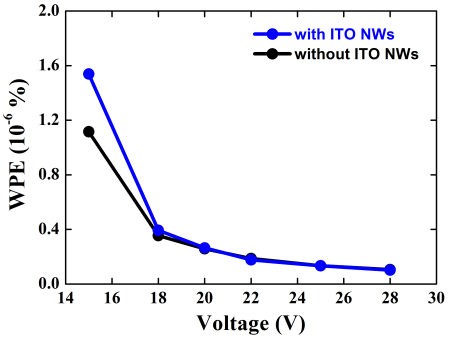

Fig. 5(c). WPEs of Si NC LEDs with and without ITO NWs.

4 CONCLUSION

A new technique for improving the optical and electrical properties of Si NC LEDs by employing ITO NWs was investigated. The I-V characteristics, light output power, and WPE of Si NC LEDs with ITO NWs was enhanced compared to those of Si NC LEDs without ITO NWs. This was attributed to an enhancement in the current spreading property of the ITO transparent layer and a decrease in the dynamic resistance of the whole Si NC LED.

ACKNOWLEDGEMENTS

This work was supported by the Converging Research Center Program through the Converging Research Headquarter for Human, Cognition and Environment funded by the Ministry of Education, Science and Technology (Grant Code: 2011K000655).

REFERENCES

[1] W. L. Ng, M. A. Lourenço, R. W. Gwilliam, S. Ledain, G. Shao, and K. P. Homewood, Nature 410, 192 (2001).

[2] M. A. Green, J. Zhao, A. Wang, P. J. Reece, and M. Gal, Nature 412, 805 (2001).

[3] B. Gelloz, T. Shibata, and N. Koshida, Appl. Phys. Lett. 89, 191103 (2006).

[4] L. Pavesi, L. Dal Negro, C. Mazzoleni, G. Franzò, and F. Priolo, Nature 408, 440 (2000).

[5] R. Huang, H. Dong, D. Wang, K. Chen, H. Ding, X. Wang, W. Li, J. Xu, and Z. Ma, Appl. Phys. Lett. 92, 181106 (2008).

[6] L. Pavesi and D. J. Lockwood, Silicon Photonics: Silicon fundamentals for photonic applications. Heidelberg, Berlin (2004).

[7] M. C. Beard, K. P. Knutsen, P. Yu, J. M. Luther, Q. Song, W. K. Metzger, R. J. Ellingson, and A. J. Nozik, Nano Lett. 7, 2506 (2007).

[8] D. Timmerman, J. Valenta, K. Dohnalová, W. D. A. M. De Boer, and T. Gregorkiewicz, Nature Nanotech. 6, 710 (2011).

[9] M. L. Brongersma, A. Polman, K. S. Min, E. Boer, T. Tambo, and H. A. Atwater, *Appl. Phys. Lett.* 72, 2577 (1998).

[10] M. V. Wolkin, J. Jorne, P. M. Fauchet, G. Allan, and C. Delerue, *Phys. Rev. Lett.* 82, 197 (1999).

[11] N. M. Park, C. J. Choi, T. Y. Seong, and S. J. Park, *Phys. Rev. Lett.* 86, 1355 (2001).

[12] Y. Q. Wang, Y. G. Wang, L. Cao, and Z. X. Cao, *Appl. Phys. Lett.* 83, 3474 (2003).

[13] T. Y. Kim, N. M. Park, K. H. Kim, G. Y. Sung, Y. W. Ok, T. Y. Seong, and C. J. Choi, *Appl. Phys. Lett.* 85, 5355 (2004).

[14] K. S. Cho, N. M. Park, T. Y. Kim, K. H. Kim, G. Y. Sung, and J. H. Shin, *Appl. Phys. Lett.* 86, 071909 (2005).

[15] C. Huh, K. H. Kim, J. Hong, H. Ko, W. Kim, and G. Y. Sung, *Electrochem. Solid State Lett.* 11, H296 (2008).

[16] K. Okamoto, I. Niki, A. Shvartser, Y. Narukawa, T. Mukai, and A. Scherer, Nat. Mater. 3, 601 (2004).

[17] O. Kulakovich, N. Strekal, A. Yaroshevich, S. Maskevich, S. Gaponenko, I. Nabiev, U. Woggon, and M. Artemyev, Nano Lett. 2, 1449 (2002).

[18] K. T. Shimizu, W. K. Woo, B. R. Fisher, H. J. Eisler, and M. G. Bawendi, Phys. Rev. Lett. 89, 117401 (2002).

[19] M. K. Kwon, J. Y. Kim, B. H. Kim, I. K. Park, C. Y. Cho, C. C. Byeon, and S. J. Park, Adv. Mater. 20, 1253 (2008).

[20] C. H. Lu, C. C. Lan, Y. L. Lai, Y. L. Li, and C. P. Liu, Adv. Funct. Mater. 21, 4719 (2011).

[21] K. Okamoto, A. Scherer, and Y. Kawakami, Phys. Stat. Sol. (c) 5, 2822 (2008).

[22] D. K. Schroder, Semiconductor Material and Device Characterization (Wiley, New York, 1990), pp. 147–149.